Supplementary Material for

Effect of Ligand Substitution on Zero-Field Slow Magnetic Relaxation in Mononuclear Dy(III) β-Diketonate Complexes with Phenanthroline-Based Ligands

Egor V. Gorshkov [1,2], Denis V. Korchagin [1,*], Elena A. Yureva [1,*], Gennadii V. Shilov [1], Mikhail V. Zhidkov [1], Alexei I. Dmitriev [1], Nikolay N. Efimov [3], Andrew V. Palii [1] and Sergey M. Aldoshin [1]

Contents:

Figure S1. FT-IR spectra for **1**, dmdophen (**3**) and $[Dy(acac)_3(H_2O)_2]\cdot H_2O$ (**5**).

Figure S2. FT-IR spectra for **2**, phendione (**4**) and **5**.

Figure S3. Powder X-ray diffraction pattern of polycrystalline sample for **1**.

Figure S4. Powder X-ray diffraction pattern of polycrystalline sample for **2**.

Table S1. Crystal data and structure refinement for **1** and **2**.

Table S2. Selected bond lengths (Å) and angles (°) for **1** and **2**.

Table S3. The local symmetry of Dy(III) ion for 1 and 2 defined by the continuous shape measure (CShM) analysis with *SHAPE* software.

Figure S5. Short intra- and intermolecular contacts in crystal pacing of **1** (top) and **2** (bottom).

Figure S6. Frequency dependences of the in-phase AC susceptibility (a) and Cole−Cole plots (b) for **1** at zero DC field and temperatures from 2 to 20 K in increment of 2 K.

Table S4. Best fit parameters for **1** at zero DC field.

Figure S7. Frequency dependences of the in-phase (a) and out-of-phase (b) AC susceptibility, Cole−Cole plots (c) for **1** at 10 K and indicated DC fields.

Figure S8. Field dependence of the inverse relaxation time τ^{-1} for **1** at 10 K.

Figure S9. Frequency dependences of the in-phase AC susceptibility (a) and Cole−Cole plots (b) for **1** at 1000 Oe DC field and temperatures from 8 to 20 K in increment of 2 K.

Table S5. Best fit parameters for **1** at 1000 Oe DC field.

Figure S10. Frequency dependences of the in-phase AC susceptibility (a) and Cole−Cole plots (b) for **2** at zero DC field and temperatures from 2 to 20 K.

Table S6. Best fit parameters for **2** at zero DC field.

Figure S11. Frequency dependences of the in-phase (a) and out-of-phase (b) AC susceptibility, Cole−Cole plots (c) for **2** at 10 K and indicated DC fields.

Figure S12. Field dependence of the inverse relaxation time τ^{-1} for **2** at 10 K.

Figure S13. Frequency dependences of the in-phase AC susceptibility (a) and Cole−Cole plots (b) for **2** at DC field 1000 Oe and temperatures from 8 to 20 K.

Table S7. Best fit parameters for **2** at 1000 Oe DC field.

Table S8. SINGLE_ANISO computed wave function decomposition analysis for lowest KDs of Dy(III) ions in **1** and **2**. It is shown only main (>10%) contributions.

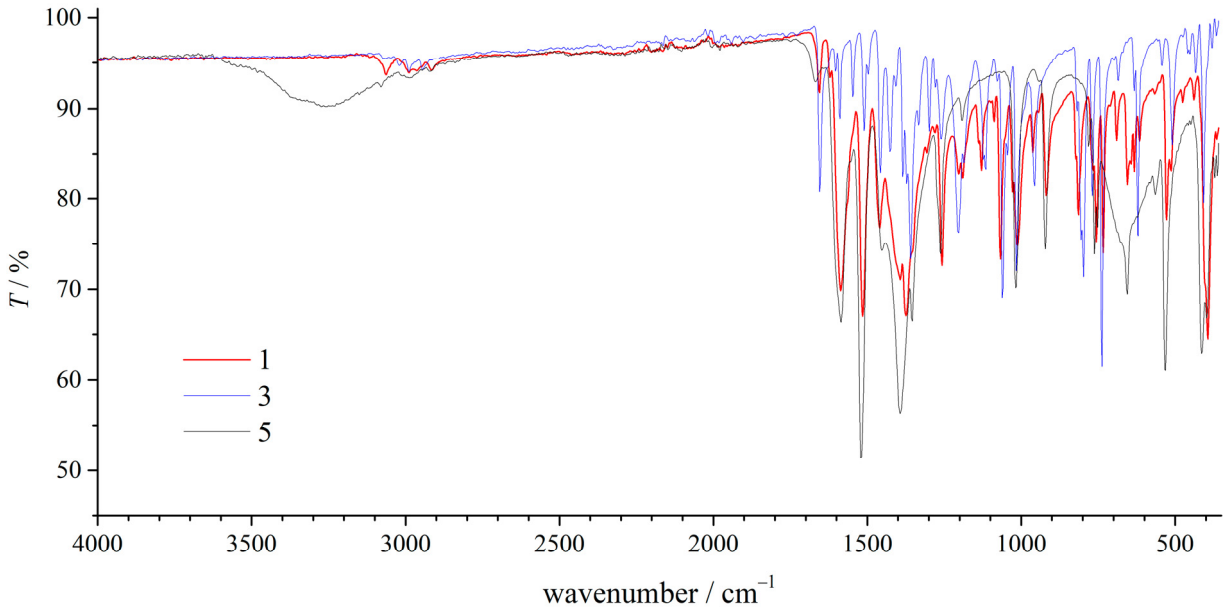

Figure S1. FT-IR spectra for **1**, dmdophen (**3**) and $[Dy(acac)_3(H_2O)_2]\cdot H_2O$ (**5**).

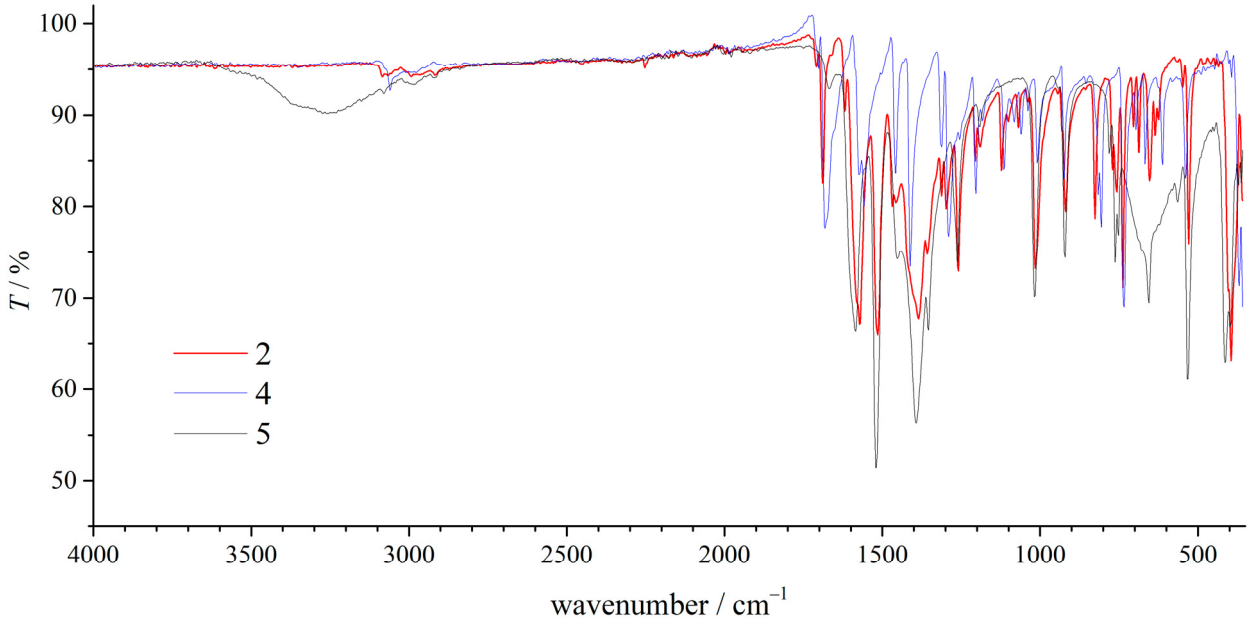

Figure S2. FT-IR spectra for **2**, phendione (**4**) and **5**.

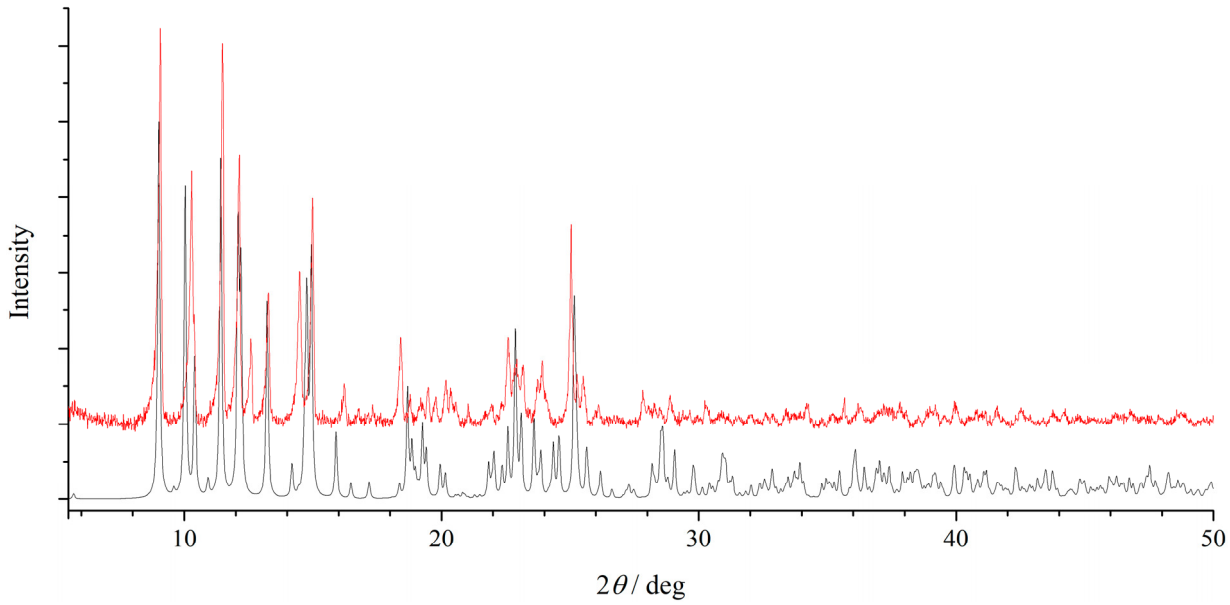

Figure S3. Powder X-ray diffraction pattern of polycrystalline sample for **1**: experimental (top) and simulated (bottom).

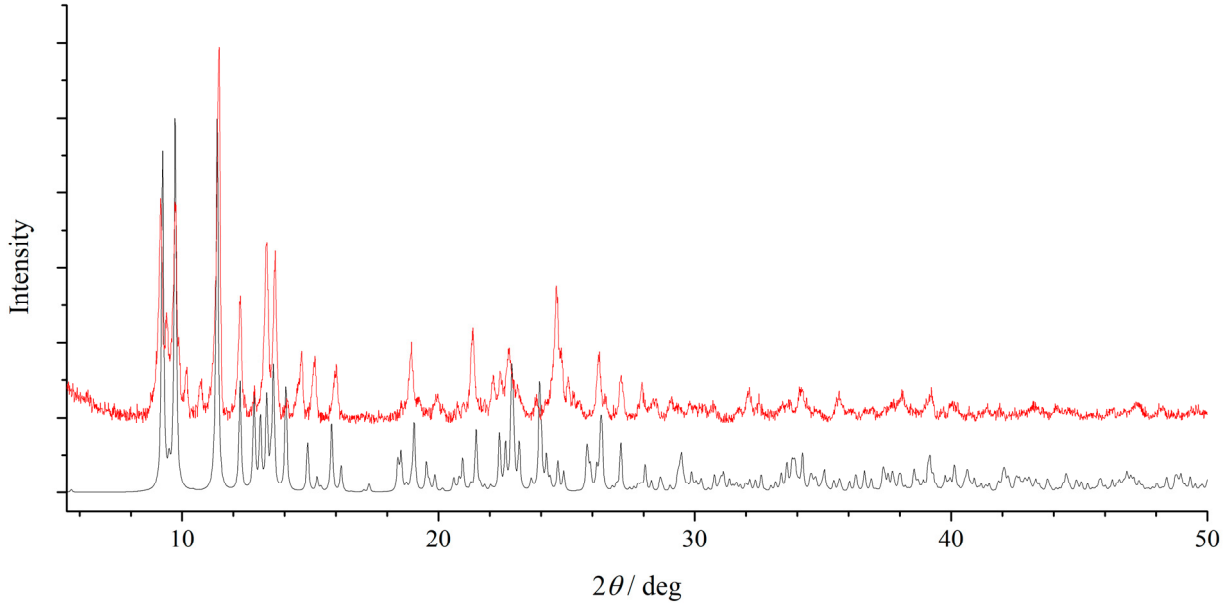

Figure S4. Powder X-ray diffraction pattern of polycrystalline sample for **2**: experimental (top) and simulated (bottom).

Table S1. Crystal data and structure refinement for **1** and **2**.

Parameters	**1**	**2**
Empirical formula	$C_{30}H_{33}DyN_2O_8$	$C_{29}H_{27}DyN_3O_8$
Formula weight, g/mol	712.08	708.03
Temperature, K	100(1)	150(1)
Crystal system; space group	Triclinic; P-1	Triclinic; P-1
a, Å	9.5844(3)	9.5998(10)
b, Å	9.9719(3)	9.6354(9)
c, Å	15.9368(5)	16.1461(8)
α, deg.	84.771(3)	104.794(6)
β, deg.	76.665(3)	94.535(6)
γ, deg.	79.950(3)	90.536(8)
Volume, $Å^3$	1457.29(8)	1438.8(2)
Z; ρ (calculated), g/cm^3	2; 1.623	2; 1.634
μ, mm^{-1}	2.616	2.651
F(000)	714	704
Crystal size, mm	0.15 x 0.10 x 0.08	0.22 x 0.12 x 0.07
θ range, deg.	2.784 to 31.672	2.823 to 26.064
Reflections collected	14726	10211
Reflections unique [R(int)]	8538 [0.0348]	5676 [0.0610]
Completeness to $\theta = 25.242°$	99.9 %	99.7 %
Number of parameters	378	371
Goodness-of-fit on F^2	1.001	1.181
Final R_1; wR_2 [$I>2\sigma(I)$]	0.0327; 0.0548	0.1080; 0.2836
R_1; wR_2 (all data)	0.0404; 0.0583	0.1247; 0.2906
$\Delta\rho_{max}$ and $\Delta\rho_{min}$, $e \cdot Å^{-3}$	1.126 and -1.095	7.875 and -3.562

Table S2. Selected bond lengths (Å) and angles (°) for **1** and **2**.

1		**2**	
Dy(1)-O(4)	2.283(2)	Dy(1)-O(5)	2.32(1)
Dy(1)-O(3)	2.298(2)	Dy(1)-O(6)	2.30(1)
Dy(1)-O(1)	2.319(2)	Dy(1)-O(2)	2.33(1)
Dy(1)-O(2)	2.319(2)	Dy(1)-O(1)	2.31(1)
Dy(1)-O(5)	2.340(2)	Dy(1)-O(3)	2.33(1)
Dy(1)-O(6)	2.345(2)	Dy(1)-O(4)	2.31(1)
Dy(1)-N(1)	2.603(2)	Dy(1)-N(1)	2.60(1)
Dy(1)-N(2)	2.632(2)	Dy(1)-N(2)	2.60(1)
O(4)-Dy(1)-O(3)	73.97(7)	O(6)-Dy(1)-O(5)	74.4(5)
O(4)-Dy(1)-O(2)	77.68(7)	O(1)-Dy(1)-O(5)	75.9(5)
O(3)-Dy(1)-O(2)	124.88(7)	O(6)-Dy(1)-O(1)	121.1(4)
O(4)-Dy(1)-O(1)	114.59(7)	O(5)-Dy(1)-O(2)	117.6(5)
O(3)-Dy(1)-O(1)	76.76(6)	O(6)-Dy(1)-O(2)	76.6(4)
O(2)-Dy(1)-O(1)	73.65(7)	O(1)-Dy(1)-O(2)	74.0(4)
O(4)-Dy(1)-O(5)	140.94(6)	O(5)-Dy(1)-O(3)	138.6(5)
O(3)-Dy(1)-O(5)	144.93(7)	O(6)-Dy(1)-O(3)	146.9(4)
O(2)-Dy(1)-O(5)	77.61(7)	O(1)-Dy(1)-O(3)	79.5(5)
O(1)-Dy(1)-O(5)	86.50(6)	O(2)-Dy(1)-O(3)	86.1(5)
O(4)-Dy(1)-O(6)	137.29(6)	O(4)-Dy(1)-O(5)	138.5(5)
O(3)-Dy(1)-O(6)	76.61(6)	O(6)-Dy(1)-O(4)	77.1(5)
O(2)-Dy(1)-O(6)	145.02(7)	O(1)-Dy(1)-O(4)	145.4(5)
O(1)-Dy(1)-O(6)	87.44(7)	O(4)-Dy(1)-O(2)	83.5(4)
O(5)-Dy(1)-O(6)	72.00(6)	O(4)-Dy(1)-O(3)	73.0(5)
O(4)-Dy(1)-N(1)	75.73(7)	O(5)-Dy(1)-N(1)	70.3(4)
O(3)-Dy(1)-N(1)	136.32(7)	O(6)-Dy(1)-N(1)	133.1(4)
O(2)-Dy(1)-N(1)	77.13(6)	O(1)-Dy(1)-N(1)	78.8(4)
O(1)-Dy(1)-N(1)	145.55(6)	O(2)-Dy(1)-N(1)	148.1(4)
O(5)-Dy(1)-N(1)	69.59(7)	O(3)-Dy(1)-N(1)	72.6(4)
O(6)-Dy(1)-N(1)	107.13(7)	O(4)-Dy(1)-N(1)	111.3(4)
O(4)-Dy(1)-N(2)	73.39(7)	O(5)-Dy(1)-N(2)	73.8(5)
O(3)-Dy(1)-N(2)	78.97(6)	O(6)-Dy(1)-N(2)	78.9(4)

O(2)-Dy(1)-N(2) 134.77(7)	O(1)-Dy(1)-N(2) 136.8(4)
O(1)-Dy(1)-N(2) 150.71(6)	O(2)-Dy(1)-N(2) 148.3(4)
O(5)-Dy(1)-N(2) 104.66(7)	O(3)-Dy(1)-N(2) 104.3(5)
O(6)-Dy(1)-N(2) 71.10(7)	O(4)-Dy(1)-N(2) 71.6(5)
N(1)-Dy(1)-N(2) 62.59(6)	N(1)-Dy(1)-N(2) 62.3(4)

Table S3. The local symmetry of Dy(III) ion for **1** and **2** defined by the continuous shape measure (CShM) analysis with *SHAPE* software [26, 27].

				1	**2**
1	OP-8	D_{8h}	Octagon	30.864	30.119
2	HPY-8	C_{7v}	Heptagonal pyramid	21.796	22.284
3	HBPY-8	D_{6h}	Hexagonal bipyramid	15.895	16.874
4	CU-8	O_h	Cube	9.843	10.217
5	**SAPR-8**	**D_{4d}**	**Square antiprism**	**0.679**	**0.543**
6	TDD-8	D_{2d}	Triangular dodecahedron	2.405	2.216
7	JGBF-8	D_{2d}	Johnson gyrobifastigium J26	15.749	16.245
8	JETBPY-8	D_{3h}	Johnson elongated triangular bipyramid J14	28.574	28.233
9	JBTPR-8	C_{2v}	Biaugmented trigonal prism J50	3.027	2.699
10	BTPR-8	C_{2v}	Biaugmented trigonal prism	2.414	2.090
11	JSD-8	D_{2d}	Snub diphenoid J84	5.121	5.129
12	TT-8	T_d	Triakis tetrahedron	10.698	11.057
13	ETBPY-8	D_{3h}	Elongated trigonal bipyramid	24.828	24.531

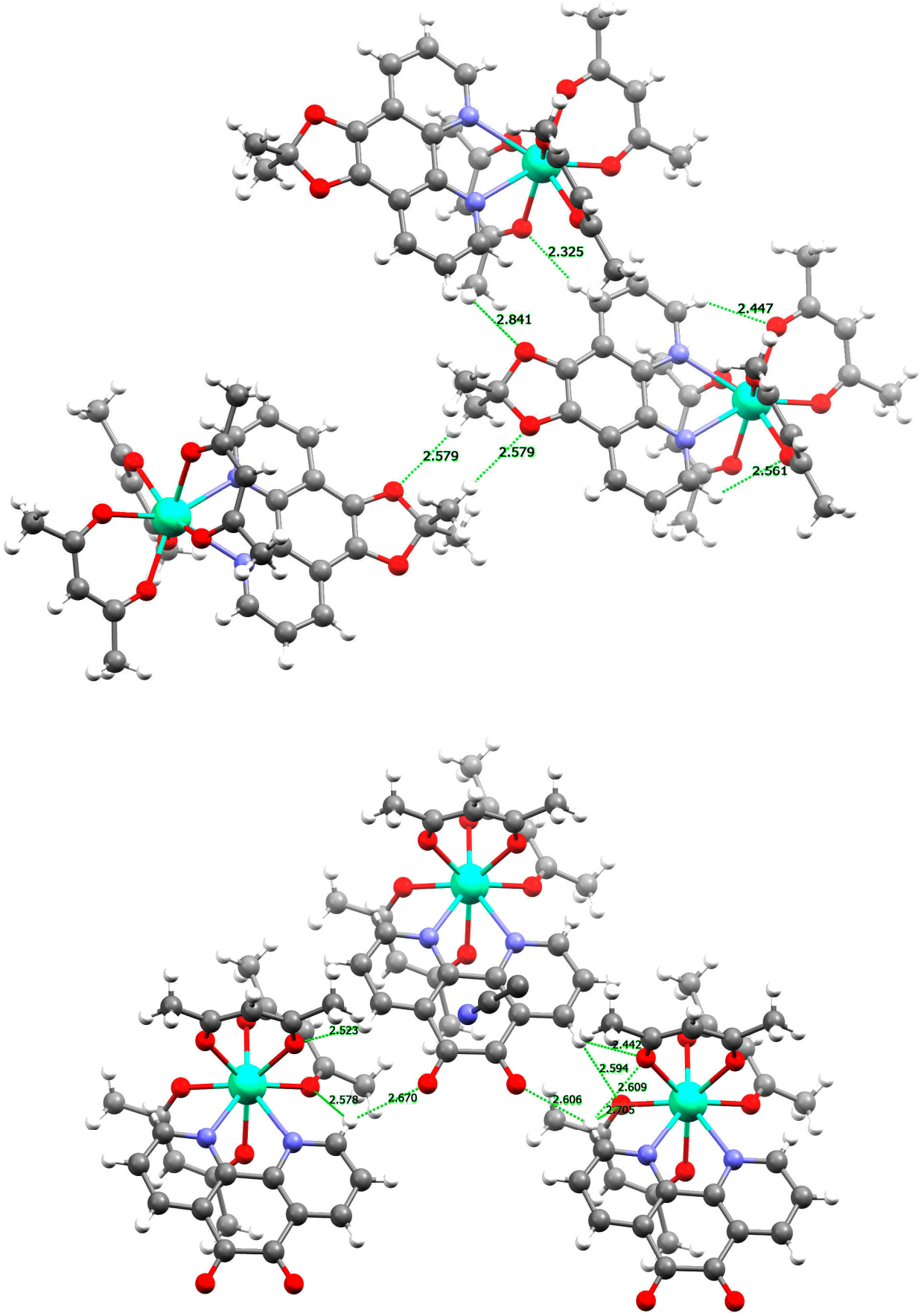

Figure S5. Short intra- and intermolecular contacts in crystal pacing of **1** (top) and **2** (bottom).

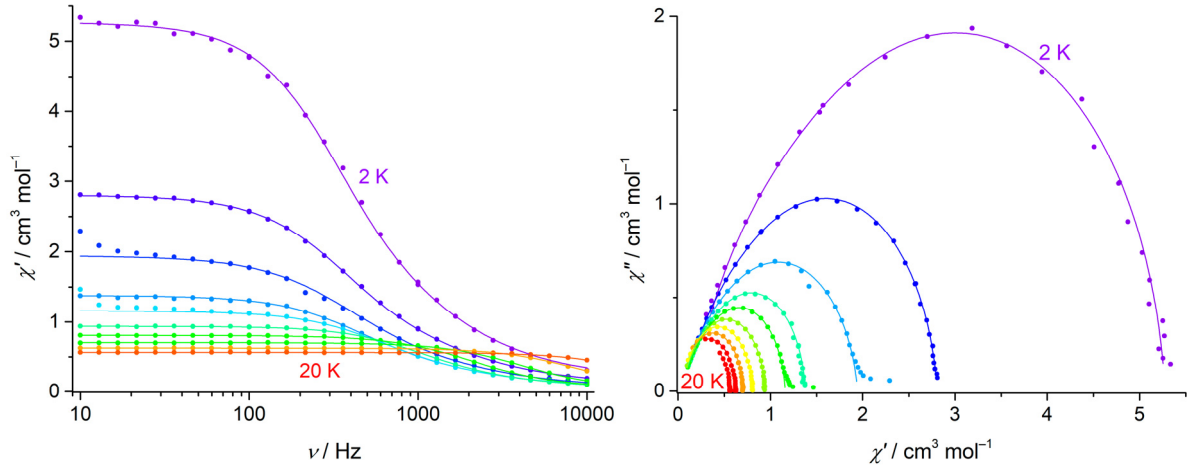

(a) (b)

Figure S6. Frequency dependences of the in-phase AC susceptibility (a) and Cole−Cole plots (b) for **1** at zero DC field and temperatures from 2 to 20 K in increment of 2 K. Dots are experimental data; solid lines indicate fit data within the Debye model with parameters listed in Table S4.

Table S4. Best fit parameters for **1** at zero DC field.

T, K	χ_S, cm^3/mol	$\Delta\chi_{T1}$, cm^3/mol	τ_1, s	α_1	$\Delta\chi_{T2}$, cm^3/mol	τ_2, s	α_2	Adj. R^2
2	1.71E-01	3.08	5.073E-04	0.032	1.81	1.273E-04	0.220	0.99941
4	8.91E-02	1.81	4.528E-04	0.056	0.86	1.020E-04	0.225	0.99971
6	4.91E-02	1.33	4.054E-04	0.088	0.49	8.337E-05	0.231	0.99870
8	4.26E-02	0.85	3.699E-04	0.034	0.49	9.391E-05	0.223	0.99951
10	5.55E-02	0.72	2.765E-04	0.032	0.39	8.169E-05	0.214	0.99978
12	4.61E-02	0.73	1.548E-04	0.033	0.16	3.334E-05	0.128	0.99993
14	5.94E-02	0.75	7.465E-05	0.055				0.99952
16	4.74E-02	0.66	3.862E-05	0.035				0.99988
17	5.82E-02	0.64	2.718E-05	0.032				0.99991
18	4.00E-02	0.58	1.810E-05	0.032				0.99979
20	2.01E-02	0.54	7.495E-06	0.038				0.99990
22	1.00E-02	0.50	2.832E-06	0.060				0.99990

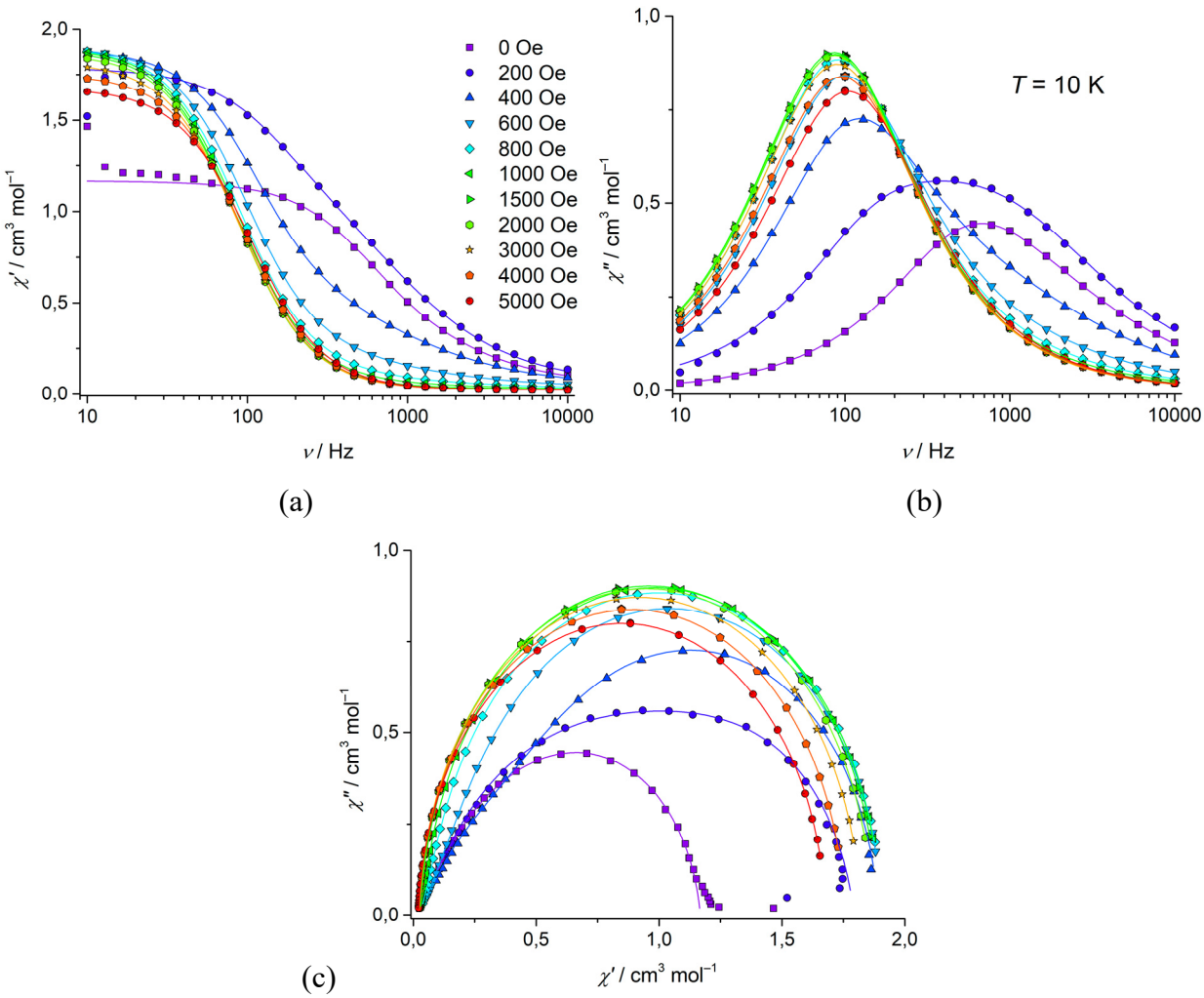

Figure S7. Frequency dependences of the in-phase (a) and out-of-phase (b) AC susceptibility, Cole−Cole plots (c) for **1** at 10 K and indicated DC fields. Symbols are experimental data; solid lines indicate fit data within the Debye model.

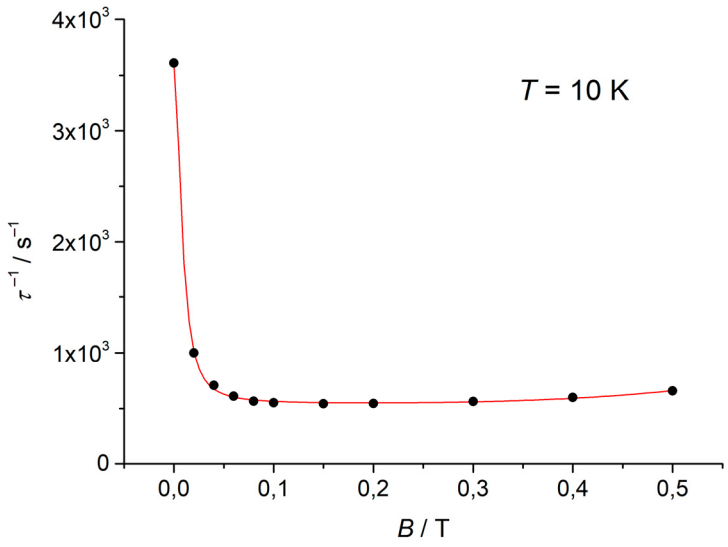

Figure S8. Field dependence of the inverse relaxation time τ^{-1} for **1** at 10 K.

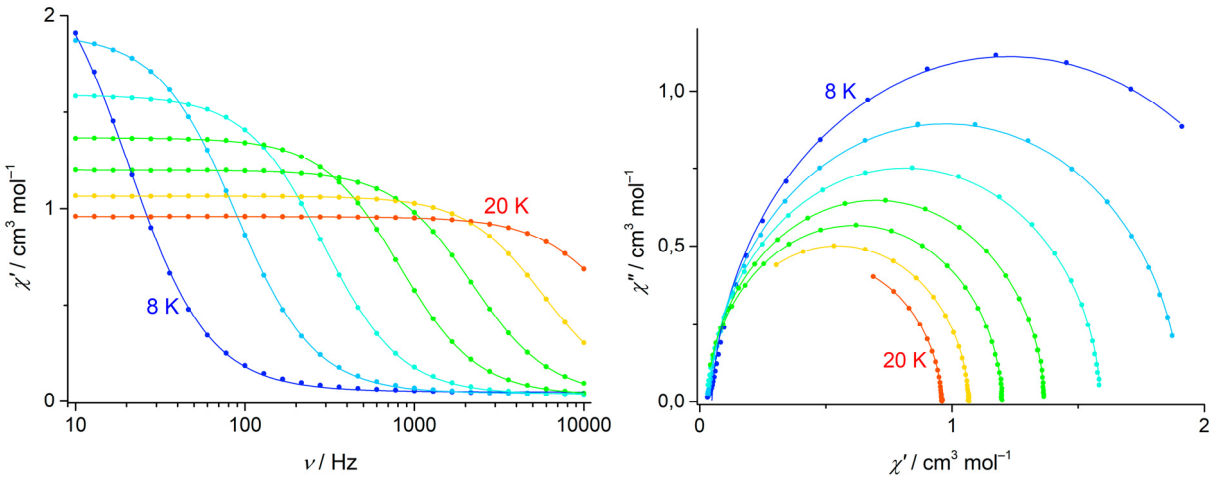

(a) (b)

Figure S9. Frequency dependences of the in-phase AC susceptibility (a) and Cole−Cole plots (b) for **1** at 1000 Oe DC field and temperatures from 8 to 20 K in increment of 2 K. Dots are experimental data; solid lines indicate fit data within the generalized Debye model with parameters listed in Table S5.

Table S5. Best fit parameters for **1** at 1000 Oe DC field.

T, K	χ_S, cm^3/mol	$\Delta\chi_T$, cm^3/mol	τ, s	α	Adj. R^2
6	5.56E-02	3.22	5.506E-02	0.085	0.99548
7	5.13E-02	2.79	1.932E-02	0.057	0.99918
8	4.81E-02	2.35	7.740E-03	0.037	0.99966
9	4.40E-02	2.08	3.580E-03	0.030	0.99984
10	3.99E-02	1.87	1.800E-03	0.027	0.99992
12	3.48E-02	1.55	5.466E-04	0.022	0.99997
14	3.06E-02	1.34	1.933E-04	0.021	0.99999
16	2.91E-02	1.17	7.299E-05	0.020	1.00000
17	3.07E-02	1.09	4.492E-05	0.018	0.99999
18	2.79E-02	1.04	2.735E-05	0.023	1.00000
19	2.88E-02	0.98	1.651E-05	0.026	1.00000
20	1.69E-02	0.94	9.689E-06	0.035	1.00000
22	9.25E-02	0.78	3.712E-06	0.049	0.99999

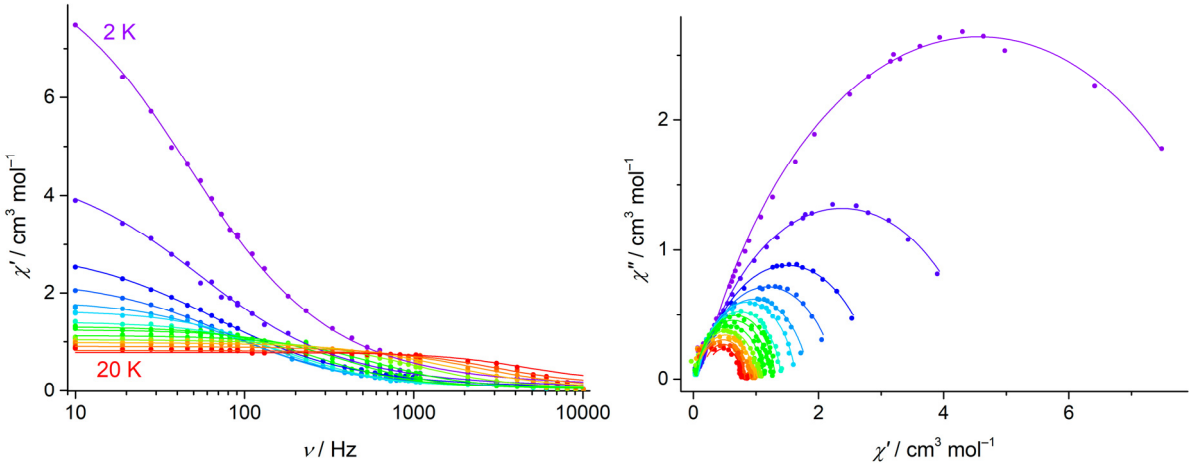

(a) (b)

Figure S10. Frequency dependences of the in-phase AC susceptibility (a) and Cole−Cole plots (b) for **2** at zero DC field and temperatures from 2 to 20 K. Dots are experimental data; solid lines indicate fit data within the generalized Debye model with parameters listed in Table S6.

Table S6. Best fit parameters for **2** at zero DC field.

T, K	χ_S, cm^3/mol	$\Delta\chi_T$, cm^3/mol	τ, s	α	Adj. R^2
2	1.04E-01	8.25	3.370E-03	0.274	0.99859
4	7.65E-02	4.16	2.960E-03	0.280	0.99787
6	6.50E-02	2.74	2.440E-03	0.273	0.99818
8	5.91E-02	2.11	2.060E-03	0.240	0.99647
10	6.80E-02	1.68	1.490E-03	0.188	0.99695
11	6.98E-02	1.47	1.080E-03	0.133	0.99375
12	6.47E-02	1.28	8.185E-04	0.118	0.99397
13	5.07E-02	1.19	5.936E-04	0.120	0.99588
14	3.07E-02	1.10	4.166E-04	0.116	0.99669
15	3.49E-02	1.01	2.727E-04	0.122	0.99617
16	3.50E-02	0.95	1.668E-04	0.142	0.99505
17	3.50E-02	0.90	1.023E-04	0.171	0.99158
18	3.75E-02	0.79	6.687E-05	0.164	0.99651
19	1.21E-01	0.64	5.217E-05	0.103	0.98800
20	1.84E-01	0.55	3.532E-05	0.091	0.99607

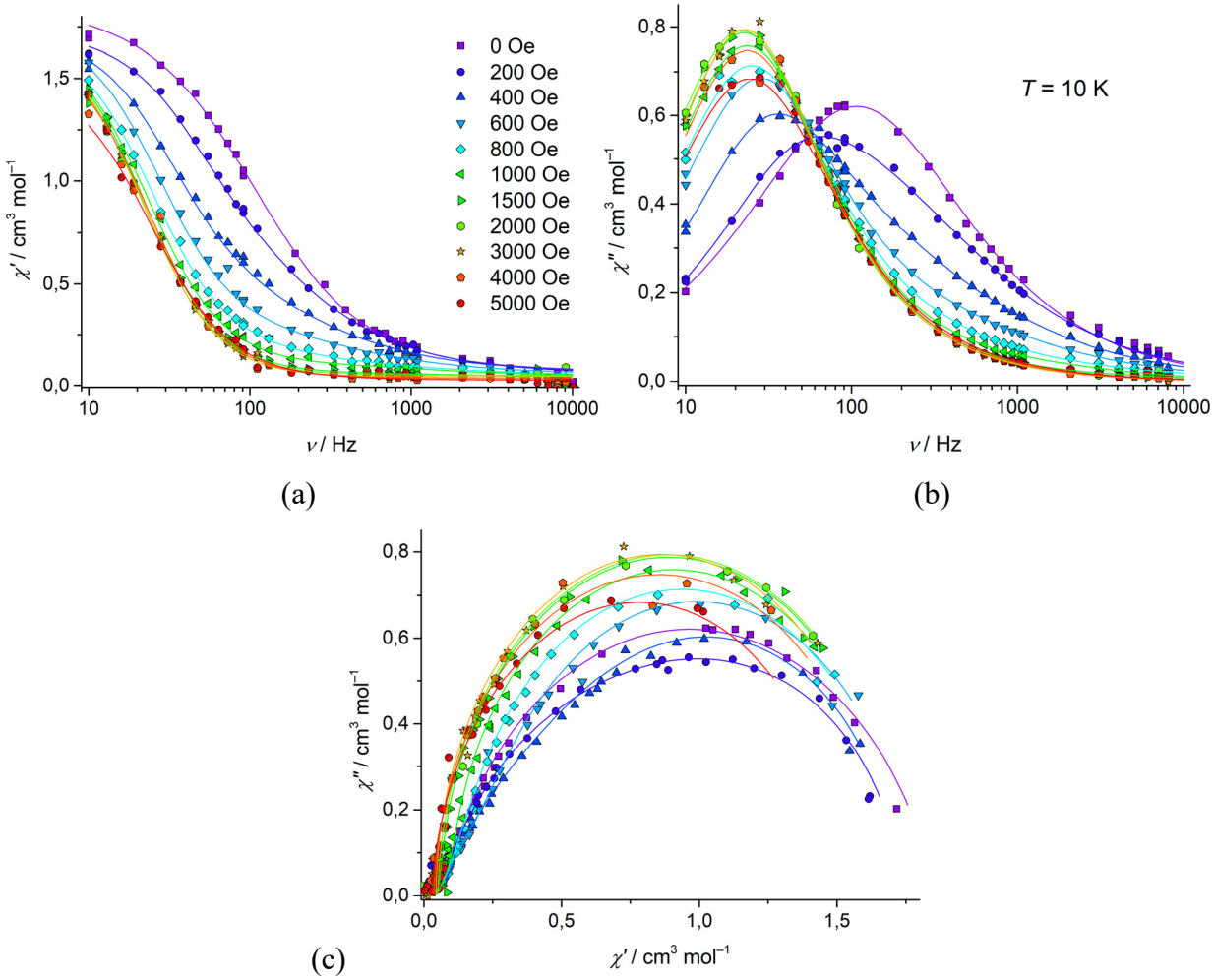

Figure S11. Frequency dependences of the in-phase (a) and out-of-phase (b) AC susceptibility, Cole−Cole plots (c) for **2** at 10 K and indicated DC fields. Symbols are experimental data; solid lines indicate fit data within the Debye model.

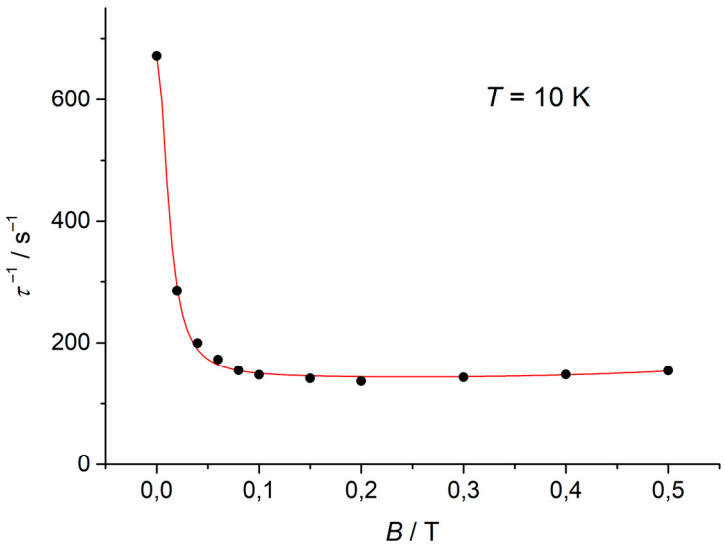

Figure S12. Field dependence of the inverse relaxation time τ^{-1} for **2** at 10 K.

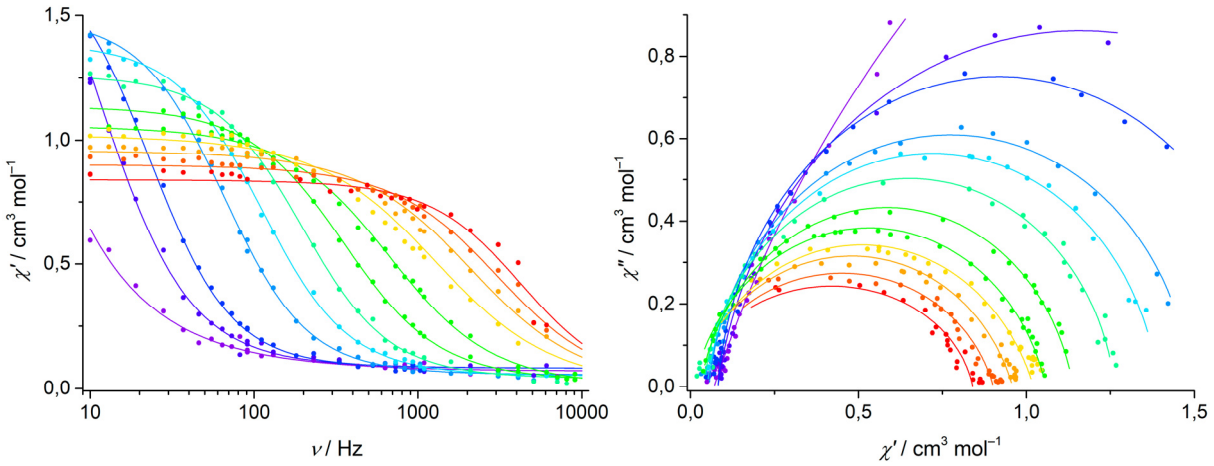

(a) (b)

Figure S13. Frequency dependences of the in-phase AC susceptibility (a) and Cole–Cole plots (b) for **2** at DC field 1000 Oe and temperatures from 8 to 20 K. Dots are experimental data; solid lines indicate fit data within the generalized Debye model with parameters listed in Table S7.

Table S7. Best fit parameters for **2** at 1000 Oe DC field.

T, K	χ_S, cm^3/mol	$\Delta\chi_T$, cm^3/mol	τ, s	α	Adj. R^2
9	8.16E-02	2.01	1.397E-02	0.098	0.99776
10	8.18E-02	1.64	6.850E-03	0.055	0.99832
12	5.52E-02	1.35	2.440E-03	0.065	0.99828
13	4.96E-02	1.28	1.430E-03	0.078	0.99784
14	3.86E-02	1.15	8.141E-04	0.082	0.99775
15	2.87E-02	1.05	4.521E-04	0.121	0.99499
16	7.12E-03	0.98	2.398E-04	0.156	0.99692
17	1.00E-03	0.97	1.251E-04	0.214	0.99027
18	1.00E-03	0.86	7.593E-05	0.191	0.99261
19	1.00E-03	0.71	5.227E-05	0.163	0.99411
20	1.00E-03	0.57	3.755E-05	0.107	0.99689

Table S8. SINGLE_ANISO computed wave function decomposition analysis for lowest KDs of Dy(III) ions in **1** and **2**. It is shown only main (>10%) contributions.

KD	**1**	**2**
1	0.927 |±15/2›	0.873 |±15/2›+0.115 |±11/2›
2	0.775 |±13/2›+0.152 |±9/2›	0.554 |±13/2›+0.229 |±9/2›
3	0.401 |±11/2›+ 0.237 |±7/2›+ 0.135 |±3/2›	0.287 |±11/2›+0.246 |±7/2›+0.116 |±13/2›+ 0.107 |±3/2›
4	0.342 |±1/2›+ 0.206 |±5/2›+0.147 |±9/2› + 0.122 |±11/2›+ 0.103 |±3/2›	0.248 |±1/2› + 0.213 |±11/2› +0.207 |±9/2›+ 0.182 |±5/2›
5	0.237 |±3/2›+ 0.191 |±5/2›+0.171 |±7/2› + 0.169|±9/2›	0.265 |±3/2› + 0.246 |±7/2› +0.165 |±5/2› + 0.117 |±9/2›+ 0.105 |±1/2›
6	0.291 |±5/2›+0.256 |±7/2›+0.163 |±3/2› + 0.143|±9/2›	0.342 |±5/2› +0.200 |±7/2› +0.197 |±3/2› + 0.103|±1/2›
7	0.412 |±1/2› + 0.304 |±3/2› +0.148 |±5/2›	0.442 |±1/2› + 0.305 |±3/2› +0.126 |±5/2›
8	0.271 |±9/2› +0.226 |±7/2› +0.209 |±11/2› + 0.126|±5/2›	0.255 |±9/2› + 0.242 |±11/2› +0.179 |±7/2› + 0.125 |±13/2›+ 0.102 |±5/2›